Near-surface and bulk short-range order in Cu_3Au

I. K. Robinson and P. J. Eng*
Department of Physics, University of Illinois, Urbana, Illinois 61801
(Received 10 March 1995; revised manuscript received 12 June 1995)

X-ray diffraction measurements of bulk short-range order (SRO) scattering from a crystal of Cu_3Au are compared with measurements of crystal truncation rods (CTR's) from a (100) surface of the same crystal. The CTR profiles have an analogous shape to the bulk SRO but, because they are confined to a narrow line in reciprocal space, are an order of magnitude more intense. Furthermore, the confinement permits exact subtraction of all sources of background, notably thermal-diffuse scattering. The CTR profile is strongly affected by the exact nature of the surface roughness, however. Our quantitative analysis shows that not only is the temperature scaling of the near-surface SRO the same as the bulk, but the numerical values of the characteristic lengths match as well.

I. INTRODUCTION

Cu_3Au is the most famous example of a binary alloy with a compositional order-disorder phase transition, and it has been widely investigated.[1–5] When $T < T_c$ the alloy has an ordered structure with simple cubic symmetry and a four-atom basis of three Cu's and one Au occupying the face-centered-cubic (fcc) sites in the cubic unit cell. When $T > T_c$ it disorders to a state in which all these fcc sites are randomly occupied, 25% by Au and 75% by Cu. In this state there remains *local* order which is structurally reminiscent of the long-range order below T_c, but with correlations in site occupation extending only over a few unit cells. This short-range order (SRO) is the analog of the magnetic fluctuations that accompany a magnetic phase transition; it is traditionally quantified by a set of short-range order parameters, each representing the probability that a given Au atom in the lattice has a Au neighbor a certain number of lattice sites away.[1–4]

The phase transition in Cu_3Au is first order, meaning that the long-range-ordered state, represented by its order parameter, disappears abruptly at T_c. The SRO is already established at this temperature and its range decreases smoothly with T above T_c. SRO can also exist below T_c in "quenched" samples that are prevented from reaching equilibrium kinetically. In such samples, the range of the SRO becomes longer with decreasing T and eventually diverges at an instability temperature, T_0, often called T_{spinodal}. If Cu_3Au did not have a first-order transition at T_c, T_0 would be its disordering temperature and the transition would be second order with divergent critical fluctuations. As with a second-order transition, a small amount of SRO also exists below T_0 and, to a diminishing extent, all the way down to $T=0$. Various studies of Cu_3Au have reported the following values of T_c: 663,[3] 667,[4] 660 K,[5] and there are two measurements of T_0: 631,[5] 629 K.[6]

This paper concerns the nature of the short-range order (SRO) near the surface of a crystal of Cu_3Au. We analyze x-ray-diffraction measurements of the crystal truncation rods (CTR's) which are sensitive to the state of the crystal surface[7] at the atomic level. The shape of the CTR for a crystal with abrupt termination at a single layer is a narrow streak of diffraction emanating from each reciprocal-lattice node along the direction of the surface normal. For an ideally terminated surface, the intensity profile along the streak is given by $I \propto 1/\sin^2 \pi L$ where L is the component of momentum transfer perpendicular to the surface (in reciprocal-lattice units). This functional form diverges (in the kinematical approximation) at every reciprocal-lattice node (bulk Bragg peak). A rough surface or one with structural relaxations gives a modified intensity profile that can be readily understood.[7]

The influence of the SRO on the CTR's of $Cu_3Au(001)$ for $T > T_c$ has a dramatic effect that we have already reported previously.[8] A large rise was found in the middle of the CTR profiles at the location in reciprocal space where it intersects the diffuse SRO scattering of the bulk. As we argued previously,[8] the origin of the extra peak in the CTR is due to coupling of the intrinsic interactions (which give rise to SRO) with *surface segregation*, the preference for one element of the binary system to lie in the surface layer. Segregation is driven by chemical forces and arises because the two elements have different binding energies in the surface. The preference of Au in the surface layer of $Cu_3Au(001)$ as a function of temperature was carefully documented by Buck, Wheatley, and Marchut[9] using low-energy ion scattering (LEIS). The effect of the intrinsic interactions is to provide a greater than average probability for Cu nearest neighbors around each Au, and vice versa. Once an excess of Au is established in the top layer, the second layer will have an excess of Cu, the third Au, and so on. In this work, we sought primarily to look more closely into the relationship with the bulk SRO scattering, and to investigate the effect of using a different sample, this one with a different composition (off-stoichiometric in the other direction), but better oriented to the crystallographic 001 plane.

II. EXPERIMENTAL METHODS

The crystal we used had a composition $Cu_{0.721}Au_{0.279}$ (Ref. 10) and had been used previously in diffraction stud-

ies of its surface.[11] The crystal used in the previous study had a composition $Cu_{0.764}Au_{0.236}$.[8] The new crystal was found to be well-oriented to its 001 face, with a miscut of 0.09° along a direction 20° away from 100. The crystal quality was not ideal, as it showed a mosaic structure with two distinct peaks 0.27° apart. The surface was prepared by sputtering with Ar^+ for 30′ at 5×10^{-5} Torr at 200 °C. The temperature was measured with a pair of chromel/alumel thermocouples spotwelded onto the clips holding the sample in place. Heating was by a filament controlled by a proportional controller which was programmed by the data-collection computer. Using this thermocouple, we determined the critical temperature, $T_c=651$ K, by careful monitoring the disappearance of one of the superstructure Bragg peaks. This is in good agreement with 648±2 K previously reported for this crystal.[10] However, it is about ten degrees below the reported values for perfectly stoichiometric Cu_3Au, listed above. Some of this may be error due to the thermocouple contacts, but T_c is expected to be depressed because of its nonideal composition.

As in the earlier work,[8] the experiments were conducted in an ultrahigh vacuum (UHV) system directly coupled to a heavy-duty x-ray diffractometer.[12] Five degrees of freedom were employed in fixing the orientation of the sample, so that the incidence angle of the beam could be controlled explicitly during measurements in all three dimensions of reciprocal space.[13] Synchrotron radiation was utilized from the National Synchrotron Light Source (NSLS) at beamline X16A. A Pt-coated toroidal focusing mirror and flat double-crystal Si(111) monochromator were used to condition the beam. The energy was chosen to be 8.9 keV, just below the Cu K absorption edge, giving $\lambda=1.388$ Å. The beamline was slit down to 1 mrad horizontally to improve the out-of-plane resolution. The diffracted beam resolution was determined by symmetric 4×4 mm slits placed 600 mm from the sample in front of the detector; this corresponds to 0.018 reciprocal-lattice units (RLU's) in the perpendicular direction. The diffraction from the crystal was indexed using the cubic convention with a lattice parameter of 3.74 Å at room temperature. We define Miller indices h and k to run parallel to the surface and L perpendicular. Alignment was achieved using two bulk {111} reflections. Separate alignments at 300 and 600° C determined the thermal-expansion coefficient to be 2.2×10^{-5} K^{-1}, and allowed us to correct all subsequent measurements for expansion of the lattice.

III. RESULTS

Upon crossing the structural phase transition in the direction of increasing temperature, only the fcc-allowed reflections of Cu_3Au are preserved, while the remaining simple cubic reflections broaden into diffuse features. The situation expected for a (001) surface of Cu_3Au is explained with the aid of Fig. 1. When $T<T_c$ (bottom panel) the CTR's diverge at every Bragg point on a simple cubic (sc) lattice while at $T>T_c$ (top panel) the situation is more complicated: half of the CTR's, with odd values of $h+k$, will vanish altogether because there are

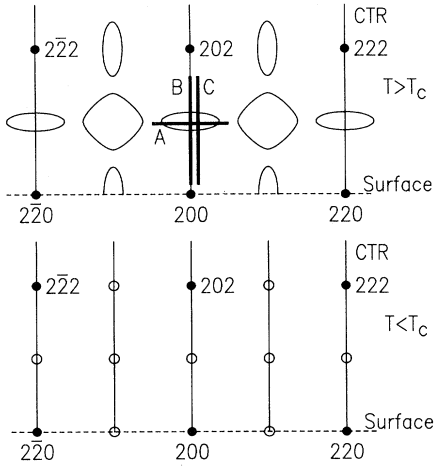

FIG. 1. Schematic diagram of a section of the reciprocal lattice of Cu_3Au showing typical intensity contours of the conventional (bulk) SRO scattering for $T>T_c$. The vertical lines indicate the locations of the crystal truncation rods (CTR's) due to terminating the crystal with a (100) face. When $T<T_c$, the SRO scattering orders into the additional Bragg peaks and CTR's indicated by open circles and lines in the lower panel. The same arrangement of peaks exists in the 1kL plane, which contains the (1,0,L) rod, expect that the pattern is shifted by one unit in both the horizontal and vertical.

no Bragg peaks left along their length, and half will remain. The profiles of the remaining CTR's will be modified because the spacing between the fcc Bragg peaks is double that of sc. The peaks of diffuse scattering due to SRO are also shown schematically in the figure; it is important to note that these even $h+k$ CTR's pass right through the SRO peaks at (hkL) positions given by $h+k$ even, $h+k+L$ odd, such as 201 in the center of the diagram.

Figure 2 shows two measurements at different temperatures (both with $T>T_c$) passing near to one of these locations of interest, the 201 point in reciprocal space. The path of this scan is designated by a bar marked A in Fig. 1. It is clear that both the sharp components of the CTR and the broad peak of the bulk SRO can be distinguished. The CTR component displays the bulk mosaic distribution of our crystal, with two grains 0.27° apart. An analogous scan through the 101 point (for example, or the equivalent point 212 seen in Fig. 1) would show only the broad component and no sign of a CTR (see below). This is easily understood with reference to the figure because the choice of a surface direction breaks the bulk cubic symmetry; the surface orientation selects one out of the three cubic axes. The CTR is not a bulk feature simply because it does not have the bulk symmetry. The shape and width of the SRO peak reproduces earlier measurements of bulk SRO scattering versus temperature.[1–4] The Fourier transform of diffuse scattering measurements like these, once extended to three dimensions and corrected for sources of background (notably thermal diffuse scattering), provides the set of Warren short-range order parameters which are usually used to quantity

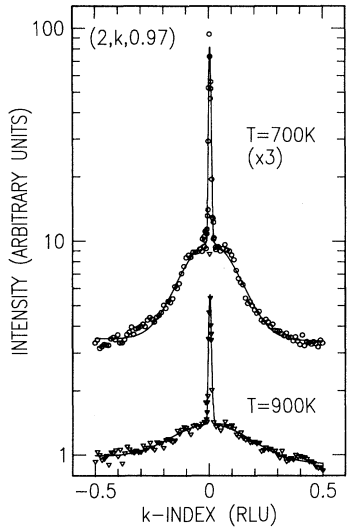

FIG. 2. Broad scan along $(2,k,0.97)$ near the 201 superstructure position at $T=700$ and 900 K. Two components are clearly seen: the broad peak is the conventional SRO scattering, while the narrow one is one point on the CTR that extends between the bulk 200 and 202 Bragg peaks.

SRO.[1–4] The data in Fig. 2 show that the heights of the CTR and bulk SRO scattering peaks can be cleanly separated because they represent distinct components of the line shape; the quantitative analysis of the temperature dependence of this kind of information will occupy the remainder of the paper.

The two-component line shape in Cu_3Au is the characteristic new observation that is attributed to the presence of a well-formed surface, since we performed our experiment in UHV. To ascertain the structural details of this surface and how they change with temperature, we need to examine the variation of the *integrated* intensity of the CTR as a function of L, the components of momentum transfer perpendicular to the surface. The interaction first removes all problems of the crystal mosaic.[3] It is clear from Fig. 2 that an accurate background subtraction is also attainable, and so the integrated intensity of the CTR can be isolated reliably from all forms of diffuse scattering, including the SRO scattering and thermal-diffuse scattering (TDS). In this sense, the CTR method offers a cleaner isolation of the local ordering than the traditional measurements of SRO scattering.

The integrated intensity, after applying the usual corrections for x-ray polarization and active sample area,[14] is plotted versus L as the square symbols at the top of Fig. 3 for a selection of temperatures. The CTR profile has the expected $1/\sin^2\pi L$ drop as it emerges from the Bragg peak at $L=0$, and is beginning to rise again towards the Bragg peak at $L=2$, but it has in addition the strong maximum in intensity near $L=1$, which is clearly visible at all temperatures.

The corresponding bulk SRO scattering at these temperatures is shown by the triangles below the CTR's in Fig. 3. These are measurements of the bulk SRO measured adjacent to the CTR, following the path indicated by the bar marked C in Fig. 1, with k displaced from the CTR center by 0.03 RLU. The circles in Fig. 3 are also measurements of the bulk SRO scattering, along a direction symmetry equivalent to C, but passing through the point (1,0,0.97) which is far from any of the CTR's. The two bulk measurements, one perpendicular to the surface and the other parallel to it, are seen to be similar in shape. They should indeed be equivalent in the bulk since they both traverse "disks" of SRO scattering (see Fig. 1) along their short axes. The intensity at both ends of the $(2,0.03,L)$ scan is also seen to increase; this is due to the contributions of TDS around the 200 and 202 Bragg peaks. The $(1,k,0.97)$ scans do not extend far enough for this to be seen.

IV. ANALYSIS OF THE CTR PROFILES

The simplest way to model the CTR profiles is to consider an otherwise ideal fcc crystal with a variable occu-

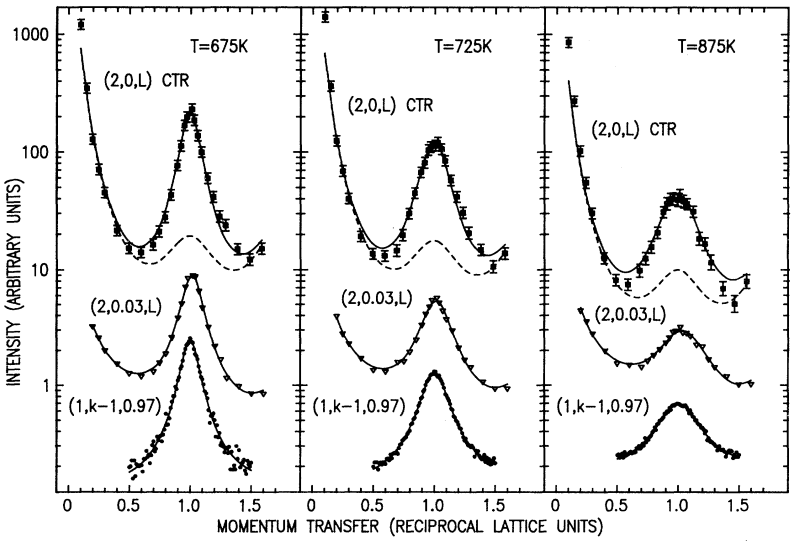

FIG. 3. Top (squares): integrated intensity profiles of the CTR's, measured along $(2,0,L)$. This scan is marked B in Fig. 1. The dashed cure is the expected shape of the CTR if there were no layerwise ordering at the surface; the peak at $L=1$ is due to the roughness, arising from the assumption of double-height steps. Middle (triangles): corresponding scans of the intensity (not integrated) through the bulk SRO scattering along the nearby position $(2,0.03,L)$, marked C in Fig. 1. Bottom (circles): bulk SRO scattering along $(1,k,0.97)$, which is a symmetry equivalent direction to $(2,0.03,L)$. The k index has been offset by one unit to facilitate comparison. All three scans would reach bulk Bragg peaks at values 0 and 2 of the horizontal scale shown. The CTR scan is perpendicular to the surface, while the k scan is parallel to the surface.

pation of each layer, and permit the occupation values to vary freely in a least-squares minimization. The perfectly random alloy can be assumed to be ideally fcc with an average scattering factor of $0.25f_{Au}+0.75_{Cu}$ for every atom.[3] Positive deviations of the occupation parameter would then correspond to enrichment of Au from the random composition, and vice versa. Enrichment to $Au_{0.5}Cu_{0.5}$ would then give an occupation parameter of 1.38, while pure Cu would appear to be 0.62. These values take into account the momentum transfer of 3.75 $Å^{-1}$ and the resonant scattering f'_{Cu} appropriate to the x-ray energy used.

The result of one such experiment, starting with all the layers set to unit occupancy except the first, is illustrated in Fig. 4. Regardless of their starting values, the refined occupancies assume a decaying oscillatory distribution. Up to 10 layers can be fit in this way, but if too many layers are given free occupancies the fit becomes unstable. It is clear from examining the figure, however, that the occupancy values are tending to follow an oscillating exponential function. Indeed, if an exponential distribution is assumed, a good fit is also obtained. If a sufficient number of layers is used, the free-occupancy model will always give a better fit, and the deviations from exponential behavior (which can be seen by close examination of Fig. 4) can become important. As we demonstrate below, the use of individual occupancy parameters is analogous to the determination of the SRO parameters from the bulk SRO scattering. With the present quality of the data, the significance of such a large number of fit parameters is somewhat doubtful, and so the free parameter model was not pursued further.

The description of variable layer occupancy is, of course, exactly the same as a common model of surface roughness,[7] which therefore must also be considered. The distinction is that the near-surface SRO effect leads to *oscillatory* occupation profiles, whereas roughness is usually described by exponential[7] or Gaussian profiles. The free-occupancy-parameter model should automatically account for both effects, which must therefore be separated *post facto*. The reason roughness is not seen in Fig. 4 is that it was accounted for directly in the calculation of the structure factor, and that the top layer occupancy was held constant (see below). Nevertheless, we must beware of potential correlations between roughness and the description of near-surface SRO.

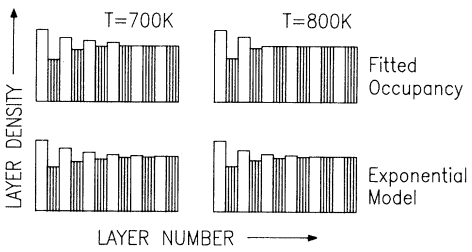

FIG. 4. Schematic picture of the two models assumed for the layer occupancy profile that were used to obtain fits to the CTR profiles. Profiles are shown for the best-fit parameters for the temperatures indicated. In each case the top layer occupancy has been fixed at a value 1.28 times the asymptotic deep-bulk value.

The CTR profile expected for the case of an exponentially damped oscillation of occupancy can be calculated explicitly. If the surface is at layer $n=0$, the occupancy of the nth layer below the surface can be written

$$\rho_n = \begin{matrix} 0\ , & n<0 \\ [1+A(-\beta_1)^n]\ , & n\geq 0\ , \end{matrix} \tag{1}$$

where A is the amplitude of the oscillation and $\beta_1(>0)$ is related to the decay length of the exponential λ by

$$\lambda = \frac{-a}{\ln(\beta_1)}\ , \tag{2}$$

where a is the layer spacing. The structure factor of the CTR is obtained by Fourier transformation of Eq. (1),

$$\begin{aligned} F_{CTR}(q) &= \sum_{n=0}^{\infty} F_0[1+A(-\beta_1)^n]\exp(iqna) \\ &= F_0\left[\frac{1}{1-\exp(iqa)}+\frac{A}{1+\beta_1\exp(iqa)}\right]\ , \end{aligned} \tag{3}$$

where F_0 is the structure factor of a single unit cell of the crystal, which is simply an atomic form factor for a primitive lattice. When surface roughness is included, in the form of a distribution of possible starting heights of the surface,[7] Eq. (3) becomes modified by an additional factor

$$F_{CTR}(q) = F_0\frac{(1-\beta)}{1-\beta\exp(-iqa')}\left[\frac{1}{1-\exp(iqa)}+\frac{A}{1+\beta_1\exp(iqa)}\right]\ , \tag{4}$$

where β represents the surface roughness in the usual way.[7] It is clear, from the opposite sign in the denominators of the two terms in Eq. (3), how an extra peak due to the imposed occupancy structure is generated at $qa=\pi$, in between the divergences of the Bragg peaks at $qa=2\pi$. The lattice spacing used in the roughness factor a' would normally be the same as a, but this need not necessarily be the case. For example, using $a'=2a$ would correspond to the situation of predominantly *double-height steps*. This may be a reasonable assumption for $Cu_3Au(001)$ because alternate layers in the ordered phase have different chemical composition, so there are two possible (001) terminations with different surface free energy. Indeed, when we used $a'=a$, we found we obtained good fits, but the parameters obtained were unrealistic: the amplitude A needed to be greater than unity. Instead we found that $a'=2a$ worked also and gave reasonable values of A. An awkward consequence of the double-height step model is that the intensity is no longer reduced by the roughness at the midpoint of the CTR at $L=1$. When $a'=2a$, the roughness function [first factor in Eq. (4)] has a period in q of just π/a, so it has two minima at $L=0.5$ and $L=1.5$ instead. This gives the appearance of an intrinsic midpoint bump, which is illustrated by the calculation of CTR profiles, including the effects of single- and double-height-step roughness in Fig. 5.

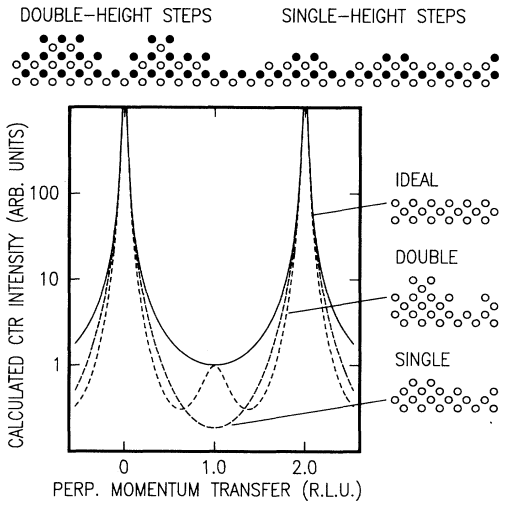

FIG. 5. Illustration of the difference between the effects of single- and double-height steps on the shape of a crystal truncation rod (CTR). Top. Atomic model of a section through an ordered $Cu_3Au(001)$ lattice showing why double-height steps might be preferred. Double-height steps expose Au-rich layers exclusively; energetically unfavorable Cu-rich terraces are avoided in this way. Au atoms are shaded. Bottom. The full curve is the function $1/\sin^2(1/2\pi L)$ corresponding to an ideally terminated face-centered-cubic (fcc) lattice of identical atoms. The calculated dashed and long-dashed curve, corresponding to statistically rough surfaces, are both obtained by multiplying this by the function $(1-\beta)^2/[1+\beta^2-2\beta\cos(n\pi L)]$, with $n=1$ corresponding to single-height steps and $n=2$ to double-height steps. Both curves are made with a roughness β parameter of 0.4 (see Ref. 7), and the structure factor of Cu_3Au has not been included in the calculation.

The full temperature range of CTR data was then fitted using Eq. (4) with the assumption of $a'=2a$. Initially, five adjustable parameters were used: the decay length parameter β_1, the amplitude A, the roughness β, an overall scale factor, and an overall Debye-Waller factor. The Debyer-Waller factor was found to have little effect, so it was fixed to the bulk value. The roughness β was more problematic because it coupled strongly with the exponential decay amplitude A. Clearly, the larger the value of β, the larger is the roughness-induced bump in the CTR profile, and the less modulation of the occupancies is needed to "fill in" the peak (see Fig. 3). Unfortunately there was also a strong correlation between β and the values of β_1. It was therefore found to be unsatisfactory to let β remain as a free parameter. We therefore assumed that the surface roughness does not change over the temperature range of the data; the potential weaknesses in this assumption are discussed in Sec. VII below. Good values of $\beta=0.27\pm0.03$ and $A=0.285\pm0.016$ were obtained from measurements of the CTR profile for $T<T_c$, where there should be minimal influence from the near-surface SRO. To model the sample in the ordered state, we simply used Eq. (4) with β_1 set to 1. The effective site occupation parameters are 0.715 and 1.285, which are within the range allowed by the composition; a small amount of site disorder is expected just below T_c.

Stable fits to the $T>T_c$ data using three parameters, scale factor, β_1, and A, were then possible up to 775 K. Above this temperature the values of A and β_1 started to become unstable, as indicated by strong parameter correlation. Since the fit values of A for $T<775$ K were essentially constant, varying by less than the error bar from the value of $A=0.28\pm0.02$, it was considered reasonable to fix A to this value for higher temperatures. In this way fits up to 875 K were obtained with values of the least-squares residual, $\chi^2<4$; above that temperature χ^2 become too large and the data were not used. $A=0.28$ corresponds to a surface layer composition of 43% Au, which agrees roughly with the values seen by LEIS over this temperature range.[9] The best fits to the data shown in Fig. 3 are drawn as solid curves, while the effect of the double-height-step roughness alone (i.e., by setting $A=0$) is shown as dashed curves. For the magnitude of the parameters needed in the fit, the extra bump due to roughness is small compared with that due to the oscillatory ordering profile. In this sense we were comfortable with the assumption of predominantly double-height steps.

Except for certain details, such as this choice of constraining the roughness parameter, this procedure is essentially the same as that used on the previous sample.[8] In both our study and the previous one, the biggest weakness in the procedure for extracting the ordering profiles from the CTR data is the assumption of exclusively double-height steps. A small admixture of single-height steps would couple strongly to the values of A and β_1 obtained. While we believe there are strong reasons for expecting double-height steps to predominate (see Sec. VII below), a minority of single-height steps is likely to be present too, and the proportion might even change with temperature. Since we found that the data could be fit well either with single- or double-height steps, and presumably with the mixture also, it was not possible to determine which situation applies in reality.

V. ANALYSIS OF THE BULK SRO SCATTERING

We have thus far shown that it is possible to model the CTR data as due to the response of the short-range order to the presence of a segregated Au layer on the outer surface. A general observation about surfaces is that the bulk physical properties, such as lattice spacings, force constants, etc., become subtly modified in the last few layers next to a free surface, so it is important for us now to establish whether the near-surfaces SRO is different from the bulk. This is a somewhat problematic task because the descriptions used in previous work on bulk Cu_3Au are in terms of the Warren SRO parameters and not in terms of correlation lengths, widely used in the analysis of other phase transitions. The historical reason for this is that a single correlation length is insufficient to describe Cu_3Au because the strength of the interactions depends strongly upon the crystallographic direction in the lattice; it is known, for example, that there are two kinds of domain wall that are the excitations involved with the disordering of the lattice at T_c. In this sense,

the set of SRO parameters at each temperature is a considerably more precise description than value of a single correlation length; the SRO parameters are technically separate order parameters of the system, although they are strongly coupled.

In the present case, we are interested in the disordering of Cu_3Au along a single direction, the (001) direction of the surface normal of our sample. It is straightforward to show from the general definition of the SRO parameters due to Warren,[3] that the *cross section* of the SRO scattering intensity is related directly through a Fourier transformation to the set of *sums* of the SRO parameters, $\alpha(lmn)$, across planes perpendicular to that direction. This permits us to write a one-dimensional (1D) description of bulk SRO starting from the general 3D case:[3]

$$I_{\mathrm{SRO}}(00L)=\sum_{n=-\infty}^{\infty}\gamma(n)\cos(\pi nL)\ , \tag{5}$$

where $\gamma(n)$ is derived by summation of the SRO parameters, $\alpha(lmn)$, over two of their indices:

$$\gamma(n)=\sum_{l,m=-\infty}^{\infty}\alpha(lmn)\ . \tag{6}$$

The coefficients $\gamma(n)$ are therefore the 1D equivalent of SRO parameters, representing the correlation in average occupancy of the nth layer with the layer at the origin. Since the occupancy is the order parameter in Cu_3Au, the function $\gamma(x/a)$ is the same thing as the conventional 1D correlation function. Equation (5) is nothing more than a restatement of the standard Fourier relationship between correlation function and intensity.

We carried out a numerical evaluation of the sums in Eq. (6) for the SRO parameters taken from the literature.[4] Only values out to $\alpha(631)$ are available, so the result is rather approximate, especially for $n=5$ and 6. It is nevertheless clear that the $\gamma(n)$ coefficients for Cu_3Au alternate in sign with n at all temperatures, and appear to follow a damped oscillatory pattern, approximately following the exponential relationship:

$$\gamma(n)=(-\gamma_0)^{|n|} \tag{7}$$

with the value of $\gamma_0(>0)$ becoming smaller as temperature increases, diminishing from 0.80 ± 0.05 at 669 K to 0.63 ± 0.11 at 958 K.

Inserting the assumed form of Eq. (7) into Eq. (5) gives a simple expression for the bulk SRO scattering:

$$I_{\mathrm{SRO}}(00L)=\frac{1-\gamma_0^2}{1+\gamma_0^2+2\gamma_0\cos(\pi L)}\ . \tag{8}$$

To the extent that Eq. (7) holds, this is the expected shape of the bulk SRO scattering along a (001) direction in reciprocal space. We therefore used Eq. (8) to fit the measurements of bulk SRO scattering in Fig. 3. We note that the function has a period of 2 RLU in L, and reaches maxima at $L=1,3,5\ldots$ and minima at $L=0,2,4\ldots$. This is correct for the $(2,0,L)$ line as well as $(0,0,L)$, as Fig. 1 shows. Equation (8) does not, however, account for the TDS around the Bragg peaks at $L=0,2,4\ldots$, so this must be added in to fit the data correctly. The $(2,0.03,L)$ data, where the TDS tail is clearly visible, were fit to Eq. (8) plus $1/L^2$ and $1/(2-L)^2$ functions of adjustable height to obtain the fits shown in Fig. 3. The χ^2 values were mostly between 1 and 2 and all smaller than 2.5. The $(1,k,0.97)$ data were fit directly to Eq. (8) without TDS, making the substitution $k=L+1$. In both cases a linear background function was included as well. This fitted background was small, positive and varied only a little with temperature. The only adjustable parameters were the value of γ_0, a peak height, a center position, a TDS height, two background parameters and an overall scale factor. The fact that Eq. (8) fits our delta reasonably well, justifies the assumed form of the decay of correlations in Eq. (7).

We note that Eq. (8) is a familiar expression. It is the same expression as the square modulus of the right-hand term in Eq. (3). It is also the standard function used to fit the diffraction line shapes of structures with stacking disorder,[15] or indeed rough surfaces.[7] It is a periodic function which rises to a Lorentzian-shaped peak in the middle of each zone of reciprocal space. The SRO scattering in Cu_3Au is so broad in reciprocal space that the overlap from one zone to the next is important, and so must be modeled comprehensively rather than using a single Lorentzian. In the limit of long correlation lengths (narrow peak), the usual relationship between an exponentially decaying correlation function and a Lorentzian line shape is upheld (in 1D). The overlap of the peaks, particularly at high temperatures, is the reason why a simple Lorentzian cannot be used to fit the bulk data, and why we use Eq. (8) instead.

VI. DISCUSSION

We are now finally in a position to make a comparison between the characteristic lengths in the near-surface region and the bulk. Figure 6 shows the variation of the

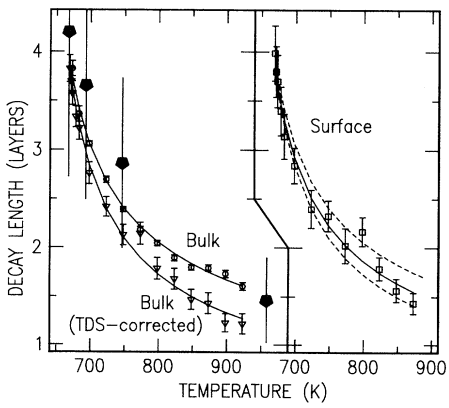

FIG. 6. Temperature dependence of the SRO correlation lengths for the bulk and near-surface region, as determined by fitting the conventional SRO scattering and CTR profiles, respectively. The solid curves are the fits that give straight lines on log-log plots (see Fig. 7), and the two bulk curves have been copied to the surface panel as dashed curves for comparison. The filled symbols are values calculated from published values of $\alpha(lmn)$ from Bardhan and Cohen (Ref. 4).

SRO decay length λ, obtained via Eq. (2) from the fit values of β_1 and γ_0 as a function of temperature. Three curves are included: the near-surface decay length from the analysis of the CTR integrated intensity (squares in Figs. 3 and 6), the bulk decay length obtained by fitting Eq. (8) to the wide scans of the bulk SRO at 101 (circles in Figs. 3 and 6), and the bulk decay length obtained from the scans along (2,0.03,L) adjacent to the CTR where the TDS has been fitted as well (triangles in Figs. 3 and 6). As mentioned above, the value of λ for the CTR (surface) data was very sensitive to the choice of constraints used in the fitting. When different values of the roughness, β, were used, the effect was to rescale the value of λ by an appreciable factor, getting 35% smaller when β was increased to 0.4. Similarly, holding A at some other value than 0.28 led to rescaling, 30% larger for a value of 0.2.

Several other bulk curves were generated using different measurements, different fitting techniques [using Eq. (4) with the bulk data, for example] and different constraints on the parameters, but always reproduced one or the other of these two curves, within error. The biggest variation arose from whether or not the TDS was accounted for in the analysis, giving the two distinct bulk curves shown in Fig. 6. The values of λ obtained from analysis of the published SRO parameters[4] are also consistent with these data. From the $\alpha(lmn)$'s we obtained $\gamma(n)$ through Eq. (6), γ_0 through Eq. (7), then λ through Eq. (2), and have included them in Fig. 6. Their large uncertainties arise not from the original data themselves but from the series truncation effects and the rough fitting to Eq. (7). They agree with our curves within error, however. We note parenthetically that it was correcting for the effects of TDS (and Compton scattering) that differentiated the various early studies of SRO parameters in Cu_3Au.[1,2] It is clear there is less difference between the near-surface and bulk data than there is between the two bulk measurements, both in the absolute value and the temperature dependence.

The expected relationship between correlation length and temperature in mean-field theory is that λ should vary as a power of the temperature differences from the *instability* temperature T_0:[8,16]

$$\lambda=\lambda_0\left[\frac{T-T_0}{T_0}\right]^{-\nu}. \tag{9}$$

The first-order phase transition temperature T_c does not appear explicitly, but simply cuts off the accessible temperature range, because of the appearance of the Bragg peak of the ordered phase, but it is reasonable to expect T_0 to remain below T_c by a fixed amount: the spinodal and phase-transition curves track each other in the composition/temperature phase diagram. The two published values of T_c-T_0 are 24 K (Ref. 5) and 34 K.[6] Our measured value of T_c was 651 K, so we take our initial estimate of T_0 to be $651-24=627$ K using the value from Ref. 5. To determine the exponent ν, we plot $\log_{10}(\lambda)$ vs $\log_{10}(T/T_0-1)$ in Fig. 7. Both near-surface and bulk data give reasonable straight lines with $\nu_{surf}=0.52\pm0.05$ and $\nu_{bulk}=0.56\pm0.05$.

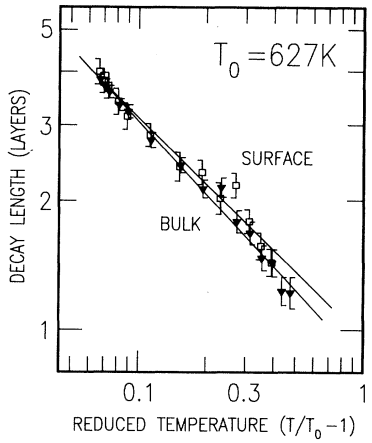

FIG. 7. Log-log plots of surface (open squares) and bulk (filled triangles) decay lengths versus reduced temperature, $t=1-T/T_0$, where T_0 has been chosen to be the literature value for the bulk instability temperature (Ref. 5). The regression fit line through the surface points has a slope of -0.52 ± 0.05; the line through the bulk points has a slope of -0.56 ± 0.05.

If instead we attempt to fit the near-surface SRO decay length to Eq. (9) and optimize all three coefficients, λ_0, T_0, and ν, we obtain $T_0=626\pm9$ K and $\nu_{surf}=0.51\pm0.05$, very close to the values above. The error in the determination does not include any of the systematics of constraining in β, which makes a large difference as explained above. Because of its large uncertainty, we are therefore unable to claim to favor one published value of T_0 over the other, although our value is consistent with either Ref. 5 or 6. Most importantly, we are able to claim consistency with the value of $\nu=\frac{1}{2}$, predicted by mean-field theory.[16]

VII. SUMMARY

This paper reports the observation and quantitative analysis of rodlike diffraction features which are due to short-range order (SRO) near the surface of Cu_3Au. The features are narrow in cross section (Fig. 2) and broad along the direction of the surface normal (Fig. 3). Their connection with the surface is beyond dispute from symmetry arguments. Their connection with SRO is somewhat enigmatic, as the sharp sectional profiles suggest order extending over hundreds of angstroms. The component of the system that imparts the order in this problem, of course, is the *surface,* which has atomically flat regions of this size. Because the surface segregation favors Au preferentially in the top layer, there is a mechanism for coupling to the SRO. SRO is described by conditional probability functions on a local scale; a Au atom has a greater-than-average probability of being surrounded by Cu than Au, and so on for more distant neighbors. These conditional probabilities for each neighbor in the lattice at each temperature are the so-called SRO parameters, $\alpha(lmn)$. The existence of SRO implies an effective interaction between the neighbors, in the sense that two

unlike (nearest) neighbors have a lower configurational energy than two like neighbors. Therefore the segregated Au layer at the surface favors, via this SRO interaction, a preference for Cu in the second layer, Au in the third layer, and so on.

The phase of the SRO is effectively *pinned* to the surface. Locally ordered regions, separated hundreds of angstroms apart across the surface, are nevertheless maintained in vertical registry with each other by their mutual relationship to the surface. They therefore diffract coherently and give rise to rodlike diffraction features that are sharp in cross section and broad perpendicular to the surface.

In detail the situation is a little more complicated because there are four sublattices in the Cu_3Au system, corresponding to the four possible origins of the SC ordered Cu_3Au unit cell within the fcc average lattice. These sublattice configurations are shown schematically at the top of Fig. 8. Each has a different translation of the SC lattice relative to the fcc one. Above T_c in the disordered state, when only local order is present, all four of these sublattices are occupied in close proximity to each other. A "snapshot" taken of the crystal at $T > T_c$ would reveal

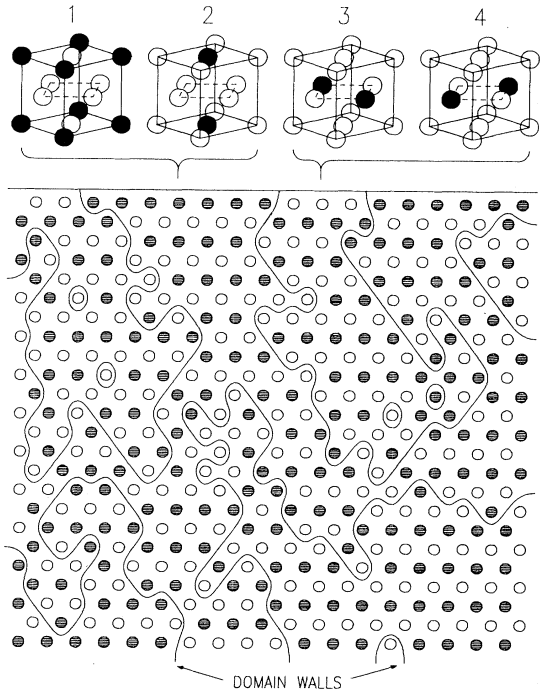

FIG. 8. Sketch of a snapshot of an instantaneous configuration of Cu_3Au showing the proposed origin of the surface-pinned SRO when segregation of Au is present. The four possible sublattices are indicated at the top. Domain walls separating sublattices 1 and 2 from 3 and 4 are indicated in the bottom panel; other domain walls are omitted for clarity. Circles in the lattice are shaded to rows of atoms of composition $Au_{0.5}Cu_{0.5}$ and left blank for pure Cu, without attention to the order along the row. The picture was generated using a Monte Carlo simulation of the 2D Ising model with antiferromagnetic nearest-neighbor interactions. Only the composition of the top layer was frozen to represent the segregation.

tiny domains, separated by domain walls, with a size distribution centered around the SRO decay length defined above. It is known that there are two types of domain wall with slightly different energy, separating pairs of sublattices with different relative displacement.[2] The domain-wall structure fluctuates in time as Cu and Au atoms interchange by diffusion in the lattice. At a (001) surface two of the four sublattices are preferred because of the segregation effect; if the top of the cubes in Fig. 8 represents the surface, then sublattices 1 and 2 have 50% Au in the surface layer, while sublattices 3 and 4 have 100% Cu. In the ordered phase of bulk Cu_3Au, long-period superstructures of domain walls are known to exist,[17] and manifest themselves in domain-wall structures at the surface;[18] such modulations are not necessarily required to disappear at $T = T_c$. When segregation is present, the domain-wall arrangement will then be biased to allow a greater number of domains with sublattice 1 and 2 to exist at the surface.

The connection between the domain walls and the surface segregation is shown schematically in the lower half of Fig. 8. When $T > T_c$ an instantaneous snapshot of the fluctuating crystal would show all the atoms at or close to lattice sites, but with their chemical identity determined by the short-range order. We have simulated this in Fig. 8 using a 2D Ising model for $T > T_c$. The instantaneous configuration of the lattice can always be divided up into domains belonging to the different sublattices by inscribing domain walls as shown. In fact only half of the domain walls are shown: those between domains 1 or 2 and domains 3 or 4 because the question of order in the direction parallel to the surface is not important to the discussion. At another moment in time the domain walls will have moved as a result of the temporal fluctuations. Our simulation has been biased by fixing the identity of the atoms in the top layer with disproportionately large proportion of $Cu_{0.5}Au_{0.5}$ rows of atoms, which therefore fixes the locations of the domain walls at the surface. The system then responds through its (antiferromagnetic) nearest-neighbor interactions in layers below the first. This causes a bending of the domain walls near the surface as they thread down into the bulk, with the effect of "squeezing out" domains 3 and 4 near the surface. The resulting (layer-averaged) concentration distribution will therefore oscillate and show a disproportionately large fraction of Au in the top layer with a corresponding reduction in the second layer.

The most general way to fit the observed intensity distributions along the CTR's is to fit individual occupancy parameters for each layer in the structure, and indeed good fits were obtained (as in Fig. 4), especially at high temperatures where the number of layers needed is not too great. This accounts for both the near-surface SRO and the roughness automatically. To obtain a simple overall thermodynamic description of the system, we used a reasonable approximation to this model by using a constant, independently measured roughness and fitting a *damped exponential* layer-occupation function, for which the structure factor was derived explicitly in Eq. (4). Nevertheless, the multiple occupancy model is more general, and, in principle, contains more information than a

single length. In fat the values of the layer occupancies can be shown to be linearly related to the $\gamma(n)$, or the 1D projection of the SRO parameters, $\alpha(lmn)$, as mapped using Eq. (6). The values of $\gamma(n)$ obtained from the published $\alpha(lmn)$ (Ref. 4) do indeed show a distinct nonexponential behavior, with $|\gamma(1)|$ smaller than expected for example, and this roughly corresponds to the deviations from ideal exponential decay visible in Fig. 4. If the short-range interactions in Cu_3Au were strictly Ising-like, with all interactions zero beyond nearest neighbor, the SRO parameters would fall off exponentially, and $\gamma(n)$ would obey Eq. (7) exactly. The deviation from exponential decay is a measure of the importance of interactions beyond the first neighbor, and hence of the extent to which there are multiple length scales in the problem.

One surprise that emerged from the analysis was that it was necessary to assume that most of the surface roughness was caused by double-height steps. This assumption has a profound effect on the shape of the CTR due to roughness alone, in the absence of any ordering, as we saw in Fig. 5. Double-height steps are a reasonable assumption given the simultaneous presence of Au segregation and the SRO, which favors Au in layers two lattice spacings apart. The proper characterization of the roughness is the main limitation of this work: it is perfectly reasonable to expect a *mixture* of single- and double-height steps to exist, and this will strongly affect the fitting parameters, including the exponent ν. Another possibility, which would produce an equivalent effect on the diffraction as a majority of double-height steps, is that (single-height) steps could be bunched into pairs, to yield a small fraction of the energetically less favorable Cu-terminated terraces, and a large fraction of Au-rich terraces. Because of the strong coupling between the Au segregation and the step distribution on the surface, we might imagine *both* to change with temperature in a concerted way, further complicating the analysis. We note that the double-height step hypothesis could be readily tested by a room-temperature scanning-tunneling microscope experiment on $Cu_3Au(001)$.

The overall conclusion of this study is that there is no observable difference in the principal characteristic decay length of short-range correlations (or its temperature-dependence above T_c) between the near-surface region of $Cu_3Au(001)$ and the bulk. The behavior seen for the near-surface region agrees well with that observed in our previous experiment,[8] and demonstrates that the surface effect is not sensitive to the exact chemical composition of the crystal.

ACKNOWLEDGMENTS

We thank K. S. Liang for the loan of the sample, R. Schuster for help with the measurements, and both for helpful discussions about Cu_3Au. We thank H. Reichert and H. Dosch for helpful discussion in the early stages of this work and for introducing us to the Cu_3Au problem. The NSLS is supported by the U.S. DOE under Grant No. DE-AC012-76CH00016. The work was supported by the University of Illinois Materials Research Laboratory under DOE Grant No. DEFG02-91ER45439.

*Present address: CARS, University of Chicago, 5640 South Ellis, Chicago, IL 60637.

[1]J. M. Cowley, Phys. Rev. **77**, 669 (1950); J. Appl. Phys. **21**, 24 (1950).

[2]S. C. Moss, J. Appl. Phys. **35**, 3547 (1964).

[3]B. E. Warren, *X-ray Diffraction* (Addison-Wesley, Reading, MA, 1969).

[4]P. Bardhan and J. B. Cohen, Acta Crystallogr. A **32**, 597 (1976).

[5]H. Chen, J. B. Cohen, and R. Ghosh, J. Phys. Chem. Solids **38**, 855 (1977).

[6]K. F. Ludwig, G. B. Stephenson, J. L. Jordan-Sweet, J. Mainville, Y. S. Yang, and M. Sutton, Phys. Rev. Lett. **61**, 1859 (1988).

[7]I. K. Robinson, Phys. Rev. B **33**, 3830 (1986).

[8]H. Reichert, P. J. Eng, H. Dosch, and I. K. Robinson, Phys. Rev. Lett. **74**, 2006 (1995).

[9]T. M. Buck, G. H. Wheatley, and L. Marchut, Phys. Rev. Lett. **51**, 43 (1983).

[10]K. S. Liang, H. H. Hung, S. L. Chang, Z. Fu, S. C. Moss, and K. Oshima, in *Surface X-ray and Neutron Scattering,* edited by H. Zabel and I. K. Robinson (Springer-Verlag, Berlin, 1992), p. 65.

[11]S. B. Rivers, W. N. Unertl, H. H. Hung, and K. S. Liang, in *Kinetics of Phase Transformations,* edited by M. O. Thompson, M. Aziz, and G. B. Stephenson, MRS Symposia Proceedings No. 205 (Materials Research Society, Pittsburgh, 1992), p. 145.

[12]P. H. Fuoss and I. K. Robinson, Nucl. Instrum. Methods Phys. Res. Sect. A **222**, 171 (1984).

[13]E. Vlieg, J. F. van der Veen, J. E. Macdonald, and M. Miller, J. Appl. Crystallogr. **20**, 330 (1987).

[14]I. K. Robinson, in *Handbook on Synchrotron Radiation,* edited by D. E. Moncton and G. S. Brown (Elsevier, Amsterdam, 1990), Vol. III.

[15]A. Guinier, *X-ray Diffraction in Crystals, Imperfect Crystals, and Amorphous Bodies* (Freeman, San Francisco, 1963).

[16]K. Mecke and S. Dietrich, Phys. Rev. B **52**, 2107 (1995).

[17]R. S. Toth and H. Sato, J. Appl. Phys. **33**, 3250 (1962).

[18]Y. Huang and J. M. Cowley, in *Proceedings of the 52nd Meeting of the Microscopy Society of America,* edited by G. W. Bailey and A. J. Garrett-Reed (San Francisco Press, Inc., San Francisco, 1994).